tvst

Article

Expression of Rab Prenylation Pathway Genes and Relation to Disease Progression in Choroideremia

Lewis E. Fry[1,2], Maria I. Patrício[1,2], Jasleen K. Jolly[1,2], Kanmin Xue[1,2], and Robert E. MacLaren[1,2]

[1] Nuffield Laboratory of Ophthalmology, Nuffield Department of Clinical Neurosciences, University of Oxford, Oxford, UK
[2] Oxford Eye Hospital, Oxford University Hospitals NHS Foundation Trust, Oxford, UK

Correspondence: Lewis E. Fry, Nuffield Department of Clinical Neuroscience, Level 6, West Wing, John Radcliffe Hospital, Oxford, OX3 9DU, UK.
e-mail: enquiries@eye.ox.ac.uk.

Received: February 9, 2021
Accepted: May 9, 2021
Published: July 13, 2021

Keywords: choroideremia; rab escort protein 1 (REP1); inherited retinal degeneration; prenylation; fundus autofluorescence

Citation: Fry LE, Patrício MI, Jolly JK, Xue K, MacLaren RE. Expression of rab prenylation pathway genes and relation to disease progression in choroideremia. Transl Vis Sci Technol. 2021;10(8):12, https://doi.org/10.1167/tvst.10.8.12

Purpose: Choroideremia results from the deficiency of Rab Escort Protein 1 (REP1), encoded by *CHM*, involved in the prenylation of Rab GTPases. Here, we investigate whether the transcription and expression of other genes involved in the prenylation of Rab proteins correlates with disease progression in a cohort of patients with choroideremia.

Methods: Rates of retinal pigment epithelial area loss in 41 patients with choroideremia were measured using fundus autofluorescence imaging for up to 4 years. From lysates of cultured skin fibroblasts donated by patients ($n = 15$) and controls ($n = 14$), *CHM*, *CHML*, *RABGGTB* and *RAB27A* mRNA expression, and REP1 and REP2 protein expression were compared.

Results: The central autofluorescent island area loss in patients with choroideremia occurred with a mean half-life of 5.89 years (95% confidence interval [CI] = 5.09–6.70), with some patients demonstrating relatively fast or slow rates of progression (range = 3.3–14.1 years). Expression of *CHM* mRNA and REP1 protein were significantly decreased in all patients. No difference in expression of *CHML*, *RABGGTB*, *RAB27A*, or REP2 was seen between patients and controls. No correlation was seen between expression of the genes analyzed and rates of retinal degeneration. Non-sense induced transcriptional compensation of *CHML*, a *CHM*-like retrogene, was not observed in patients with *CHM* variants predicted to undergo non-sense mediated decay.

Conclusions: Patients with choroideremia, who are deficient for REP1, show normal levels of expression of other genes involved in Rab prenylation, which do not appear to play any modifying role in the rate of disease progression.

Translational Relevance: There remains little evidence for selection of patients for choroideremia gene therapy based on genotype.

Introduction

Choroideremia is an X-linked recessive inherited retinal degeneration caused by mutations in the gene *CHM* (OMIM 300390; NM_000390.4). The typical course of outer retinal degeneration in choroideremia is characterized by nyctalopia in childhood, progressive visual field constriction, and loss of central visual acuity beyond the fourth decade of life.[1–3] This corresponds to structural changes observed on fundus autofluorescence imaging[4,5] and optical coherence tomography (OCT).[6] Individuals within cohorts of patients with choroideremia demonstrate a range of phenotypic severity, however, where some patients experience a milder disease course with slower rates of degeneration compared to others with more severe disease at a similar age.[2,3,5,7,8] For some patients, slower degeneration has been correlated with residual expression of full-length *CHM* transcripts due to splicing aberrations,[7] however, for most patients, studies have been unable to explain genetic factors that may contribute to phenotypic variation.[3,9]

The *CHM* gene spans 15 exons on chromosome Xq21.2 to encode Rab Escort Protein 1 (REP1), a ubiquitously expressed 653 amino acid protein.[10,11]

REP1 is involved in the prenylation of Rab GTPases, a member of the Ras superfamily of G proteins involved in vesicle trafficking.[12] Prenylation is a post-translational modification where one or more geranylgeranyl groups are covalently attached to the C-terminus of the Rab protein. Prenylation is required for the correct cellular localization, membrane association, and protein-protein interactions of Rabs. The reaction is catalyzed by Rab geranylgeranyl transferase II (GGTase-II), comprised of an alpha subunit encoded by the *RABGGTA* gene and a beta sub-unit encoded by the *RABGGTB* gene.[13,14] Newly synthesized Rabs must be escorted from the endoplasmic reticulum and presented to GGTase-II for prenylation by REP1 or its paralogue Rab Escort Protein 2 (REP2) encoded by the retrogene *CHML* (CHM-like).[13,15] REP2 also supports the GGTase-II mediated prenylation of Rabs, although with a different but overlapping substrate specificity to REP1.[15,16] Following prenylation and activation by exchange of guanosine diphosphate (GDP) for guanosine triphosphate (GTP), Rabs are guided to their target membrane by REP proteins to undertake their functions.[13] In the retina, Rabs are important for retinal pigment epithelium (RPE) homeostasis, contributing to photoreceptor outer segment phagocytosis[17,18] and melanosome trafficking to the apical microvilli.[19–21]

The Rab prenylation deficit that arises as a result of mutations, which affect the function of REP1, is critical in the pathogenesis of choroideremia, causing alterations to vesicular trafficking,[13] disruption of melanosome maturation and movement[13] and shortening of rod photoreceptor outer segments.[22] Prenylation of the Rab family of proteins is ubiquitous within all cells, however, under-prenylation of RAB27A has been implicated in the pathogenesis of choroideremia.[16,23,24] RAB27A is prone to under-prenylation: it is prenylated at one of slowest rates of all Rabs,[16] and other Rabs are prenylated in preference to RAB27A,[24] especially when REP activity is reduced. Further, the RAB27A-REP2 complex has a lower affinity for GGTase-II than the RAB27A-REP1 complex,[16] suggesting that REP2-mediated prenylation of RAB27A may not be able to fully compensate for a lack of REP1 activity in the RPE in patients with choroideremia.

Although REP1 deficiency is the underlying cause of choroideremia, it is possible that other genes involved in the Rab prenylation pathway may influence the prenylation of Rabs, and, in turn, the rate of degeneration in choroideremia. To investigate other genetic factors in the prenylation pathway that might be associated with the observed variability in choroideremia progression, we calculated the progression rate of a cohort of patients using serial fundus autofluorescence imaging and then quantified the expression of the key prenylation genes *CHM*, *CHML*, *RABGGTB*, and *RAB27A* in fibroblasts derived from these patients. Furthermore, as recent studies have demonstrated in animal models that nonsense mediated decay of genes could lead to upregulation of gene paralogues through a new mechanism of non-sense induced transcriptional compensation,[25,26] we investigated if patients with *CHM* mutations predicted to result in nonsense mediated decay expressed upregulated levels of *CHML* mRNA.

Materials and Methods

The study was conducted in accord with the Declaration of Helsinki and received approval by the UK Research Ethics Committee (reference 15/WA/0087). Written informed consent was obtained from all participants.

Clinical Assessment

Clinical data were collected from patients with a confirmed genetic diagnosis of choroideremia with pathological variants in *CHM*. BluePeak (488 nm) 55 degrees fundus autofluorescence images were captured using the Heidelberg Spectralis confocal scanning laser ophthalmoscope (Heidelberg Engineering) on annual visits as part of natural history studies for gene therapy trials. This comprises 30 patients that were previously analyzed (but with 4 years follow-up for 5 of these patients)[5,7] and an additional 11 patients. Overall, 15 of the 41 patients had 4 years of data available for analysis. Analysis of the autofluorescence island and half-life of degeneration was performed as previously described.[7] Briefly, the area of the central contiguous of each eye was outlined manually using Heidelberg Eye Explorer (HEYEX; Heidelberg Engineering), adjusted for baseline image focal length, expressed as a percentage of the total measured 55 degrees field area, and a mean percentage area of both eyes was calculated. In two patients, only one eye was used for area measurements: the first patient received gene therapy to one eye, which was excluded, the second patient did not have images of adequate quality for analysis. An individual half-life of the mean autofluorescence area was calculated for each patient using a linear regression of the logarithm of the autofluorescence area to obtain a decay constant (λ) for each patient from the gradient of the line of best fit for that patient. Half-life ($t_{1/2}$) was subsequently calculated as $N_{(t)} = N_{(0)}e^{-\lambda t}$, where

$t_{1/2} = \ln(2)/\lambda$. All patients with less than 2 years of follow-up were excluded from half-life analysis.

Fibroblast Culture

Fifteen male patients with a confirmed molecular diagnosis of choroideremia (Supplementary Table S1) and 14 control male patients (Supplementary Table S2) with a confirmed genetic diagnosis of an inherited retinal degeneration (but normal *CHM* gene) were recruited for a skin biopsy. A 4-mm full thickness skin punch biopsy was obtained from all patients under local anesthetic. The biopsies were placed in Advanced DMEM (Gibco) supplemented with 20% fetal bovine serum (FBS), then washed with phosphate-buffered saline (PBS) prior to sectioning. The biopsies were sectioned into smaller (2–3 mm) pieces using sterile scalpel blades and forceps in drops of FBS placed in 6-well plates. The pieces were transferred into a T25 flask using forceps; the flask was then flipped upside down and 6 mL of media (Advanced DMEM supplemented with 20% FBS, 100 U/mL penicillin, 100 µg/mL streptomycin, and 2 mM L-Glutamine) was added to the bottom of each flaks (top surface). The flask was placed upside down in a humidified 37°C, 5% CO_2 incubator for 24 hours. After this period, the flasks were carefully flicked back to the original position, returned to the incubator, and left undisturbed for 7 days. Fibroblast outgrowth was monitored from day 7 onward, and media was replaced every 2 to 3 days, and the flask reached confluency. Cells were sub-cultured in Advanced DMEM supplemented with 10% FBS, 100 U/mL penicillin, 100 µg/mL streptomycin, and 2 mM L-Glutamine, up to passage 7.

Preparation of Total Cell Lysates and In Vitro Prenylation Activity

Primary fibroblasts were cultured in 6-well plates and lysates were obtained from cells between passage 2 and 5, as previously described.[27] The reactions for in vitro prenylation were set up using total cell lysate (15 µg), recombinant rat GGT-II (2 µM; Jena Biosciences, Jena, Germany), and biotin-labeled geranyl pyrophosphate (B-GPP, 5 µM; Jena Biosciences) as lipid donor in prenylation buffer. All reactions were supplemented with fresh guanosine 5′-diphosphate (GDP, 20 mM; Merck Millipore, Watford, UK), DTT (1 mM; Thermo Fisher Scientific, Loughborough, UK), and recombinant REP1 protein (2 µM, fish His-REP1; Jena Biosciences, Jena, Germany). The reactions were incubated for 2 hours at 37°C and then stopped by addition of Laemmli sample buffer.

Western Blot Analysis

Prenylation reaction products were subjected to SDS-PAGE on 10% pre-cast polyacrylamide gel (Criterion, Bio-Rad, Hertfordshire, UK), transferred to a PVDF membrane (TransBlot Turbo; Bio-Rad, Hertfordshire, UK), and blocked with blocking buffer (PBS + 0.1% Tween20 [PBST] + 3% BSA) for 45 minutes. For detection of protein expression, membranes were incubated separately using anti-beta-actin (AM4302; Thermo Fisher Scientific, Loughborough, UK; 1:30,000), anti-human REP1 clone 2F1 (MABN52; Merck Millipore, Watford, UK; 1:2,500), and anti-human CHML clone 5G4 (Sigma-Aldrich; 1:2,000) primary antibodies in blocking buffer for 1 hour under agitation. Membranes were washed 3 times for 7 minutes with Phosphate Buffered Saline with Tween (PBST), incubated with fluorescent-labeled secondary antibody (IRDye; LI-COR Biosciences, Cambridge, UK; 1:10,000) for 30 minutes in blocking buffer, washed again as before, and detected using an Odyssey Imaging System (LI-COR Biosciences). The incorporation of biotinylated lipid donor by the pool of unprenylated Rab proteins was detected by direct incubation with streptavidin (IRDye 800CW Streptavidin; LI-COR Biosciences; 1:5,000) for 30 minutes. Densitometry data analysis was performed using ImageStudio Lite software (LI-COR Biosciences).

Quantitative Polymerase Chain Reaction

RNA was extracted from cultured fibroblasts using RNeasy Mini kit (Qiagen, Germany) and cDNA prepared using SuperScript III FirstStrand kit (Thermo Fisher Scientific) according to the manufacturer's instructions. Reverse transcription quantitative polymerase chain reaction (qPCR) reactions to assess messenger RNA (mRNA) expression were performed using TaqMan-based probe assays following a 6-carboxyfluorescein–minor groove binder (FAM-MGB) design for *CHM* (exon 3/4 junction, Hs01114157_m1; Thermo Fisher Scientific), *CHML* (Hs00266202_s1; Thermo Fisher Scientific), *RABGGTB* (Hs00190183_m1; Thermo Fisher Scientific), and *RAB27A* (Hs00608302_m1;Thermo Fisher Scientific). Expression level was normalized to *GAPDH* (Hs02758991_g1; Thermo Fisher Scientific). All reactions were prepared in triplicate using TaqMan Fast Universal PCR Master Mix (Thermo Fisher Scientific) and run using the QuantStudio 7 Flex Real-Time PCR System (Thermo Fisher Scientific). The normalized fold change in gene expression for each patient was calculated relative to mean expression to control patients using the $\Delta\Delta$Ct method.

Nucleotide Alignments

To calculate the sequence identity between transcripts, the Basic Local Alignment Search Tool (BLASTn)[28] was used to query the *CHM* transcript (NM_000390.3) against the human reference sequence (RefSeq) database.

Statistical Analysis

Data were assessed for normality using the D'Agostino and Pearson test and Q-Q data plots. For qPCR data, statistical comparisons between multiples groups were conducted with a 2-way ANOVA with adjustment for multiple comparisons using the Sidak method on untransformed ΔΔCt values, with data presented as the geometric mean of $2^{-\Delta\Delta Ct}$ values normalized to control expression with 95% confidence intervals (95% CIs). Pairwise comparisons were performed using Student's *t*-test or the Mann Whitney U test for parametric and nonparametric data, respectively. For tests of correlation, Pearson correlation coefficients were calculated for parametrically distributed data, and Spearman correlation coefficients for nonparametric data. Data were analyzed using Prism version 8.0 (GraphPad).

Results

Degeneration Rates Among a Cohort of Patients with Choroideremia

Clinically, patients with choroideremia can appear to progress through their disease at different rates. We collected fibroblast samples from 15 patients with choroideremia for analysis of the expression of prenylation pathway genes and whether these correlated with disease progression. To first quantify the rate of disease progression in these patients, we used serial fundus autofluorescence imaging. Fundus autofluorescence imaging in patients with choroideremia characteristically demonstrates an area central residual autofluorescence (Fig. 1A,B) that represents the remaining RPE and correlates with the central area of retina with remaining sensitivity.[4,5,29] This well characterized method enables the rate of degeneration to be quantified by calculating the degeneration half-life of the area of the central autofluorescence island over serial measurements.[4,5,7,29]

Fundus autofluorescence areas and half-lives of fibroblast donors were analyzed within our cohort of patients with choroideremia[5,7] that now includes 41 choroideremia patients followed for up to 4 years. Consistent with previous reports, the cohort demontrated autofluorescence area loss in a pattern of exponential decay (Fig. 1C), with a mean half-life of 5.89 years (95% CI = 5.09–6.70; Fig. 1D).[5,7] Within the cohort, a range of disease severity was observed, with some patients progressing at faster or slower rates compared to the cohort mean. This provided a range of degeneration rates among fibroblast donors for correlation with gene expression data. The two patients with the longest half-lives in this cohort have been previously described to express residual full-length *CHM* transcripts,[7] but other factors contributing to degeneration rate remain unexplored.

Expression of Genes in the Rab Prenylation Pathway is Similar Between Patients and Controls

As choroideremia results in a disruption of the ubiquitous Rab prenylation pathway (see Fig. 2A), the expression of four key genes involved in this pathway were investigated (Figs. 2B, 2C) in fibroblasts derived from patients with choroideremia ($n = 15$) and controls ($n = 14$): *CHM* (NM_000390.4), *CHML* (NM_001381853.1), *RABGGTB* (NM_004582.4), and *RAB27A* (NM_004580.5).

As expected, the expression of the gene *CHM*, which encodes for the protein REP1, was significantly decreased in patients with choroideremia (choroideremia patient relative quantity [RQ] = 0.13, 95% CI = 0.04 – 0.38 vs. controls RQ = 1.0, 95% CI = 0.89 – 1.12, $P < 0.0001$; see Fig. 2B). A significant outlier with high *CHM* expression was observed in the choroideremia patient group. This patient has a pathological noncontiguous duplication in *CHM* resulting in 2 transcripts: the first comprises exons 1 to 12 without exons 13 to 15 or a termination or polyadenylation signal; the second unit arises from a duplication event and comprises the exons 1 to 2 and exons 9 to 15.[30] The primer set used in this study binds within exon 3, and so detects the expression of the first transcriptional unit. This transcript does not lead to the translation of detectable or functional REP1 protein.

Among the other genes studied, no significant differences in expression were observed between patients and controls (see Fig. 2B). This was observed for *CHML*, the *CHM*-like retrogene that encodes REP2 (RQ = 0.90, 95% CI = 0.71 – 1.17 vs. controls RQ = 1.0, 95% CI = 0.90 – 1.12; $P = 0.99$); for *RABGGTB*, which encodes the β-subunit of GGTase-II (RQ = 1.19, 95% CI = 1.01 – 1.41 vs. controls RQ = 1.0, 95% CI = 0.91 – 1.09; $P = 0.95$); and for *RAB27A*, which encodes the Ras related protein RAB27A

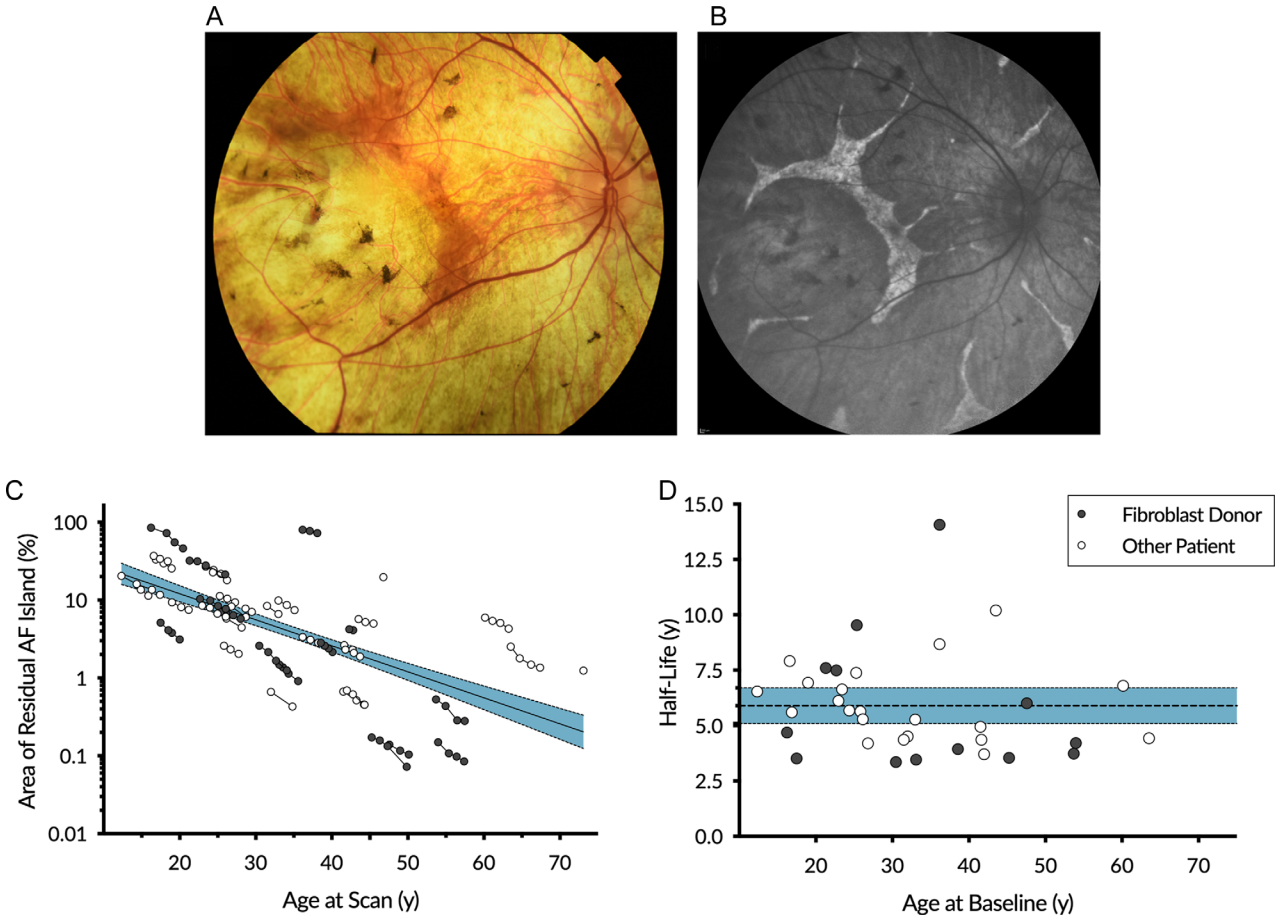

Figure 1. **Disease progression measured by autofluorescence area in a choroideremia cohort.** The typical appearance of the fundus of a patient with choroideremia seen on color imaging (**A**) and blue autofluorescence (**B**). The area of remaining autofluorescence area can be measured to follow retinal degeneration over time. (**C**) Longitudinal measurement of the progression of mean autofluorescence area remaining from 81 eyes from 41 patients. Data from fibroblast donors whose samples are used for further analysis in this study are highlighted. Consistent with previous reports, this demonstrates a pattern of exponential decay. Data is plotted on a log scale fitted with linear regression (y axis intercept = 1.751; slope = −0.033; $R^2 = 0.405$). (**D**) The half-life of degeneration of patients demonstrates variation in rates of progression across age. Half-lives calculated for patients with three or greater measurements (mean = 5.80 years, 95% CI = 5.09 − 6.70; $n = 34$). Shaded area represents 95% CI of the mean. Fibroblast donors in this study are highlighted. AF = autofluorescence.

(RQ = 0.97, 95% CI = 0.84 – 1.12 vs. controls RQ = 1.0, 95% CI = 0.92 – 1.09; $P > 0.99$).

Non-Sense Mediated Decay of *CHM* does not Lead to *CHML* Upregulation

Experiments in animal models suggest that genes subject to non-sense mediated decay can cause the upregulation of gene paralogues with sequence similarity, through a transcriptional genetic compensation mechanism.[25,26] *CHML* is an intron-less retrogene and paralogue of *CHM,* and the primary transcripts have 79.0% sequence identity. To investigate whether this genetic compensation effect occurs in humans with choroideremia, *CHML* expression was analyzed in the subgroup of patients with choroideremia with mutations in *CHM* predicted to result in nonsense mediated decay of the transcript ($n = 12$; Supplementary Table S1) relative to controls ($n = 14$). In this subgroup, there was no difference in *CHML* mRNA levels between patients and controls (RQ = 0.85, 95% CI = 0.62−1.17; $P = 0.36$ unpaired t-test). Furthermore, there was no significant correlation between these variables (Pearson $R^2 = 0.23$, $P = 0.11$) and an inverse relationship that might suggest an increase in expression of *CHML* due to non-sense induced transcriptional compensation caused by the occurrence of premature termination codons in *CHM* was not observed (Fig. 2C).

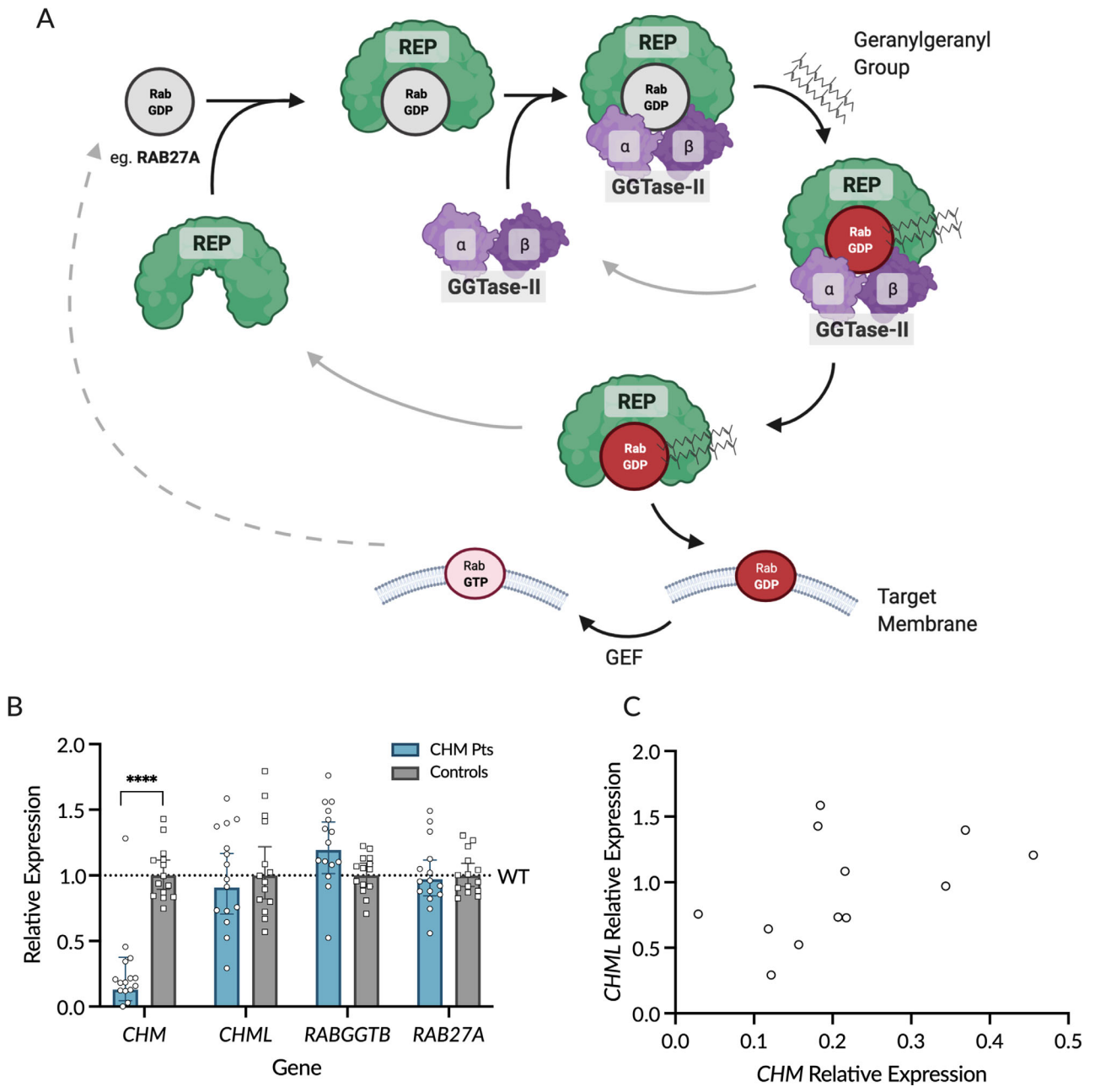

Figure 2. **Expression of genes involved in the Rab prenylation pathway.** (**A**) An overview of the Rab prenylation pathway. Newly synthesized Rabs (e.g. Ras-related protein RAB27A, encoded by gene *RAB27A*) are bound by the Rab Escort Proteins, REP1 (encoded by *CHM*) or its paralogue REP2 (encoded by *CHML*). REP proteins present Rabs to the GGTase-II heterodimer composed of α and β subunits (encoded by genes *RABGGTA* and *RABGGTB*, respectively) for prenylation. GGTase-II catalyses Rab prenylation, adding a geranylgeranyl diphosphate group to the Rab C-terminus. This allows for insertion of the Rab into the target membrane where it is activated from the guanosine diphosphate (GDP) to the guanosine triphosphate (GTP)-bound state by the guanine nucleotide exchange factor (GEF). Once activated in the target membrane, the Rab protein mediates critical functions including membrane trafficking, vesicle formation, movement, and fusion (depending on the specific Rab). Following fusion, Rab-GTP is converted back to Rab-GDP by a GTPase activating protein (GAP) and returns to the cytoplasm to bind REP (dotted line). (**B**) Expression of genes in the prenylation pathway in skin-derived fibroblasts from choroideremia patients ($n = 15$) relative to controls ($n = 14$). *CHM* expression in patients with choroideremia is significantly reduced relative to controls ($P < 0.0001$). No significant differences in expression were observed between patients and controls in the genes *CHML* ($P = 0.99$), *RABGGTB* ($P = 0.95$), or *RAB27A* ($P > 0.99$). (**C**) Expression of *CHM* plotted against *CHML* for patients with mutations predicted to result in non-sense mediated decay of the *CHM* transcript ($n = 12$). No inverse correlation between the levels of *CHML* and *CHM* expression was seen to suggest any compensational upregulation of *CHML* (Pearson $R^2 = 0.23$, $P = 0.11$).

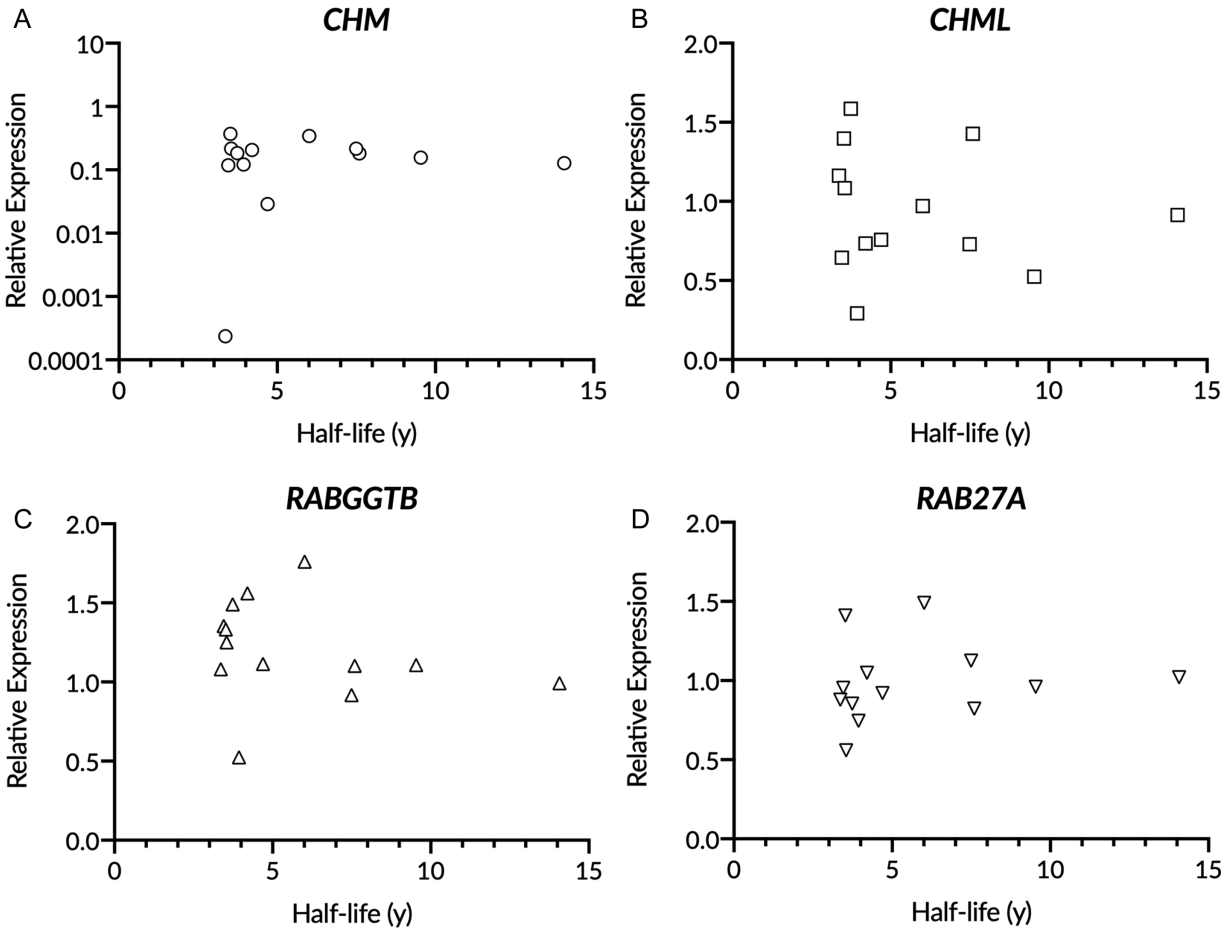

Figure 3. Expression of genes in the Rab prenylation pathways does not correlate with the rate of disease progression in choroideremia. (**A–D**) Half-life of the degeneration of autofluorescence area for patients with choroideremia ($n = 13$) plotted against relative expression of *CHM* **A** (Spearman r = 0.13, $P = 0.69$), *CHML* **B** (Pearson $R^2 = 0.01$, $P = 0.65$), *RABGGTB* **C** (Pearson $R^2 = 0.05$, $P = 0.42$), and *RAB27A* **D** (Pearson $R^2 = 0.02$, $P = 0.67$). No significant correlations were observed.

Expression of Rab Prenylation Genes are not Correlated to Degeneration Half-Life

Although no overall differences were observed between patients with choroideremia and controls in the expression of the Rab prenylation pathway genes, variation in the expression of these genes was observed within both patient cohorts. To investigate if the expression levels of each gene might contribute to the rate of disease progression in individual patients with choroideremia, the relationship between gene expression and autofluorescence area half-life was explored among the 13 patients for whom both fibroblasts and longitudinal imaging data were available. Across all four genes (*CHM*, *CHML*, *RABGGTB*, and *RAB27A*) no correlation was observed between the level of gene expression and degeneration half-life (all $P > 0.05$; Fig. 3).

REP Protein Expression and the Level of Unprenylated Rab Proteins are not Related to Rate of Degeneration

Fibroblast cell lysates from patients with choroideremia and controls were also assessed for REP1 and REP2 protein expression, as well as prenylation activity using an in vitro biotinylated prenylation assay that quantifies the unprenylated cytosolic Rab pool. Patients with choroideremia demonstrated markedly diminished REP1 protein expression (Fig. 4, see Supplementary Table S1) relative to controls (Choroideremia RQ = 0.04, 95% CI = 0.02 – 0.06 vs. controls RQ = 1.0, 95% CI = 0.77 – 1.22, $P < 0.0001$). Cell lysates from patients with choroideremia also demonstrated a significantly increased pool of unprenylated Rabs in the prenylation assay, consistent with a reduced REP1-mediated prenylation

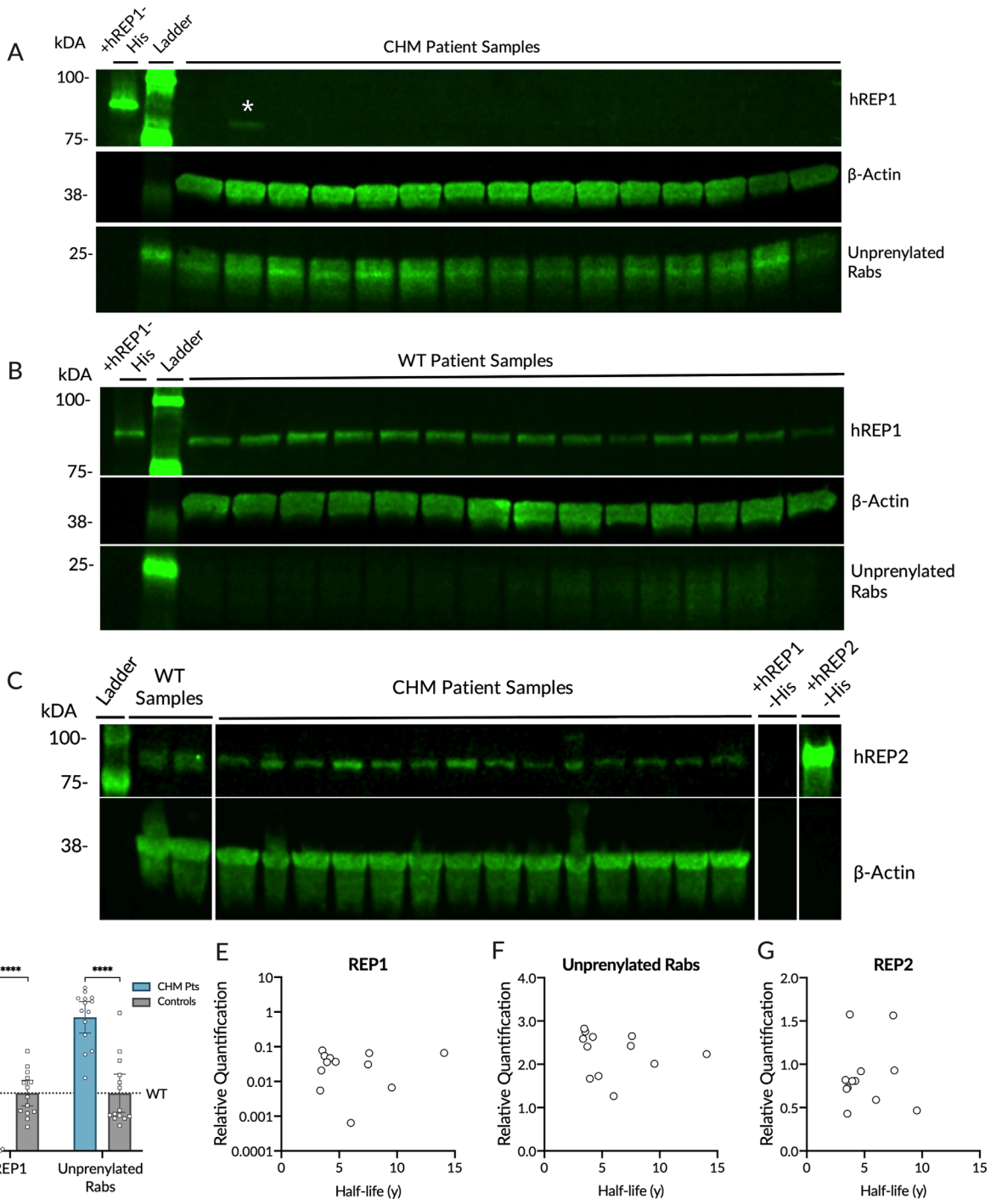

Figure 4. **Quantification of REP expression and level of unprenylated Rab proteins.** (**A**) Fibroblast lysates from patients with choroideremia were assessed for human REP1 expression (hREP1) and the level of unprenylated Rabs following an in vitro prenylation reaction. In the in vitro prenylation assay, unprenylated Rabs incorporate a biotin-labeled analogue of geranylgeranyl-pyrophosphate, allowing the quantification of the pool of unprenylated Rabs by the level of biotin incorporated during the reaction. Each lane represents an individual patient (see Supplementary Table S1 for patient details). The lane labeled with an asterisk (*) shows detection of a truncated REP1 band in the patient with an in-frame deletion of exons 2 and 3 (c.117_314del; p.R40_S105del). (**B**) Fibroblast lysates from control patients assessed for hREP1 expression and levels of unprenylated Rabs. (**C**) Fibroblast lysates from patients with choroideremia (see Supplementary Table S2 for patient details) and controls assessed for hREP2 expression. Detection of hREP2 requires loading of a larger quantity of protein per lane, leading to smearing of actin bands. (**D**) Quantification of hREP1 expression and the pool of unprenylated Rabs by densitometry in patients with choroideremia and normalized to expression in controls. REP1 expression in choroideremia patients is significantly reduced compared to controls ($P < 0.0001$, Student's *t*-test). The pool of unprenylated Rabs is significantly increased in patients with choroideremia ($P < 0.001$, →

←

Mann Whitney test). **(E, F)** Plot of relative quantification of REP1, unprenylated Rabs, and REP2 in patients with choroideremia relative to controls and their half-life of the degeneration of mean autofluorescence area. The rate of choroideremia progression measured by autofluorescence half-life is not correlated with REP1 expression (Pearson $R^2 = 0.02$, $P = 0.66$), the quantity of unprenylated Rabs (Spearman r = −0.4, $P = 0.19$), and REP2 expression (Spearman r = 0.14, $P = 0.66$).

activity (RQ = 2.31, 95% CI = 2.04 – 2.59 vs. controls RQ = 1.0, 95% CI = 0.67 – 1.32, $P < 0.001$; see Fig. 4).[27] No significant correlation was detected between the rate of degeneration and the level of residual REP1 expression (Pearson $R^2 = 0.02$, $P = 0.66$) or pool of unprenylated Rabs (Spearman r = −0.4, $P = 0.19$) quantified by band densitometry of the Western blot (see Fig. 4). Furthermore, REP2 expression was detected in all patients with choroideremia (see Fig. 4, see Supplementary Table S2), but no significant correlation was detected between the level of REP2 expression and rate of retinal degeneration (Spearman r = 0.14, $P = 0.66$).

Discussion

The rate of retinal degeneration and vision loss can vary substantially among patients with choroideremia; however, it remains unclear what contributes to this range of phenotypes in most patients. With gene therapy treatments for choroideremia currently being evaluated in advanced clinical trials,[31–36] understanding whether genetic factors influence the disease course is important as this may influence the selection of patients for, or the response of patients to, gene therapies.

The reduction of prenylation of Rab GTPases associated with REP1 deficiency (or sometimes loss-of-function) is crucial in the pathogenesis of choroideremia,[13] with the most affected Rabs being RAB27A[23,24] and RAB38.[24] Loss-of-function variants in *CHM* reduce REP activity, however, multiple other factors contribute to Rab prenylation rates. The expression of REP2 likely compensates for deficiencies in REP1 expression in the prenylation of Rab proteins elsewhere in the body,[37] but this appears insufficient in the eye, leading to gradual RPE and photoreceptor degeneration. The current study investigated whether the expression levels of other genes in the Rab prenylation pathway that act together with REP1 may act as modifiers in the choroideremia disease course. Within the patient cohort studied, there does not appear to be an association between severity of phenotype and *CHML*, *RAB27A*, *RABGGTB*, mRNA, or REP2 protein levels in patients with choroideremia. To our knowledge, this is the first study to explore potential correlations between severity of disease progression and the expression of Rab prenylation pathway genes or prenylation activity.

This study used fundus autofluorescence imaging to characterize disease progression, a highly reproducible method for quantifying RPE degeneration over time in choroideremia.[4] This study includes a total of 41 patients followed with autofluorescence imaging; a larger cohort and with an increased length of longitudinal follow-up (up to 4 years) in 15 patients to improve the accuracy of autofluorescence half-life calculations beyond previously published reports.[5,7] Consistent with previous findings, the autofluorescence area reduction over time followed a pattern of exponential decay with a mean half-life of 5.89 years (95% CI = 5.09 – 6.70). Previous studies that reported longer half-lives ranging from 6.3 to 8.7 years included younger patients in earlier stages of the disease[5,7] and used cross-sectional data[4] or shorter length of follow-up,[5,7] which may account for the differences in half-lives observed. Our image analysis method was able to clearly identify patients, for whom fibroblast samples were available, that progressed at slower or faster rates than the cohort mean.

The influences on phenotypic variability in patients with choroideremia have now been investigated at multiple levels, however, it remains difficult to establish a clear relationship between genotype and phenotype in choroideremia. At a DNA variant level, there appears to be little correlation between the *CHM* variant and disease severity or age-of-onset.[3,9,38] At a protein level, most variants are null mutations causing absence of REP1 and the few missense mutations are predicted to result in a nonfunctional protein.[39] Some associations have been established at the RNA level. An analysis of patients with *CHM* with noncanonical splice site mutations demonstrated the preservation of low levels of wildtype *CHM* transcripts that correlated with slower disease progression.[7] It has also been suggested that slower disease progression is seen in patients with any detectable *CHM* mRNA expression. However, it is difficult to comment on these results as little information was included as to how the RNA expression studies were conducted.[2] The current study extends these RNA analyses to demonstrate that there is little variation in the expression of related genes in the preny-

lation pathway in patients with choroideremia that might account for the individual phenotypic variations seen.

Recent work has described a phenomenon whereby paralogous genes may be upregulated when a gene is subject to non-sense mediated decay.[25,26] *CHML* is an intron-less retrogene paralogous to *CHM* that was inserted in chromosome 1 during mammalian evolution. We did not find any upregulation of *CHML* relative to controls in 11 patients with choroideremia with pathogenic variants expected to cause non-sense decay of the *CHM* transcript (see Supplementary Table S1). This transcriptional adaptation mechanism is not expected to occur for alleles that completely fail to be transcribed, such as might be expected in alleles with large deletions of *CHM* or the promoter region. If transcriptional adaptation was occurring in choroideremia by *CHML* upregulation, patients with non-sense mutations might be expected to have milder disease than those with large deletions; however, this is not the case.[3,9]

Why the eye is selectively affected in choroideremia when REP1 expression is ubiquitous is a longstanding area of inquiry. Current evidence suggests that RPE may be more susceptible to a deficit in Rab prenylation that disrupts an intricately balanced and highly active vesicular trafficking process required for the phagocytosis of photoreceptor outer segments and melanosome maturation and movement.[13] One limitation of this study is that it relied on patient-derived skin fibroblasts (due to obvious inherent difficulties with obtaining retinal tissue), thus the findings may not be representative of the prenylation activities in the eye. However, as Rab prenylation occurs in all cells, cultured primary fibroblasts still represent a useful ex vivo model, and under-prenylation of Rabs was consistently detected in choroideremia patient-derived cells compared with controls. Future studies using induced pluripotent stem cell (iPSC)-derived retinal organoids or RPE from patients with choroideremia may provide further insight into these results.

The underlying cause for phenotypic variability in choroideremia remains unclear, with possibilities including more complex genetic interaction or variations in prenylation in the retina not investigated here, environmental factors, and stochastic effects.[3] The absence of any correlation between disease severity and activity of other key enzymes in the prenylation pathway raises the possibility that REP1 deficiency may cause choroideremia through another hitherto undefined mechanism. The results of this study continue to support the understanding that REP1 deficiency is the primary defect in choroideremia, and the rationale for *CHM* gene replacement therapy. Our results add to the conclusions of previous work that there is, to date, little evidence for the exclusion or inclusion of specific patients for retinal gene therapy based on genotype.[3]

Acknowledgments

The authors would like to thank all study participants and the Eye Research Group Oxford (ERGO) at the Oxford Eye Hospital.

Funding: This research was funded by support from the NIHR Oxford Biomedical Research Centre, Fight for Sight UK (reference 1718/1719), the Rhodes Trust, Medical Sciences Internal Fund University of Oxford, the Royal College of Surgeons of Edinburgh, the North Harbour Club Charitable Trust and the Amar-Franses & Foster-Jenkins Trust, and the Wellcome Trust (216593/Z/19/Z). The funders had no role in the design and conduct of the study; collection, management, analysis, and interpretation of the data; preparation, review, or approval of the manuscript; and decision to submit the manuscript for publication.

Conflicts of Interest: M.I.P. and R.E.M. are named inventors on a patent owned by the University of Oxford relating to prenylation assays in choroideremia. The authors have no other relevant affiliations or financial involvement with any organization or entity with a financial interest in or financial conflict with the subject matter discussed in this work.

L.F., J.J., and M.P. had full access to all the data in the study and takes responsibility for the integrity of the data and the accuracy of the data analysis.

Author Contributions: Study conception and design: L.F., J.J., M.P., and R.E.M. Design of experiments and data acquisition: M.P., J.J., and K.X. Analysis and interpretation: L.F., J.J., M.P., K.X., and R.E.M. Primary drafting of manuscript: L.F. Critical review and editing: L.F., J.J., M.P., K.X., and R.E.M All co-authors have reviewed and approved of the manuscript prior to submission.

Disclosure: **L.E. Fry,** None; **M.I. Patrício,** Prenylation Assay (P); **J.K. Jolly,** None; **K. Xue,** None; **R.E. MacLaren,** Prenylation Assay (P)

References

1. MacDonald IM, Russell L, Chan C-C. Choroideremia: new findings from ocular pathology and review of recent literature. *Surv Ophthalmol.* 2009;54(3):401–407.

2. Di Iorio V, Esposito G, De Falco F, et al. CHM/REP1 transcript expression and loss of visual function in patients affected by choroideremia. *Investig Opthalmology Vis Sci*. 2019;60(5):1547.
3. Freund PR, Sergeev YV, MacDonald IM. Analysis of a large choroideremia dataset does not suggest a preference for inclusion of certain genotypes in future trials of gene therapy. *Mol Genet Genomic Med*. 2016;4(3):344–358.
4. Jolly JK, Edwards TL, Moules J, Groppe M, Downes SM, MacLaren RE. A qualitative and quantitative assessment of fundus autofluorescence patterns in patients with choroideremia. *Invest Ophthalmol Vis Sci*. 2016;57(10):4496–4498.
5. Aylward JW, Xue K, Patricio MI, et al. Retinal Degeneration in choroideremia follows an exponential decay function. *Ophthalmology*. 2018;125(7):1122–1124.
6. Aleman TS, Han G, Serrano LW, et al. Natural history of the central structural abnormalities in choroideremia: a prospective cross-sectional study. *Ophthalmology*. 2017;124(3):359–373.
7. Fry LE, Patrício MI, Williams J, et al. Association of messenger RNA level with phenotype in patients with choroideremia: potential implications for gene therapy dose. *JAMA Ophthalmol*. 2020;138(2):128–135.
8. Khan KN, Islam F, Moore AT, Michaelides M. Clinical and genetic features of choroideremia in childhood. *Ophthalmology*. 2016;123(10):2158–2165.
9. Simunovic MP, Jolly JK, Xue K, et al. The spectrum of CHM gene mutations in choroideremia and their relationship to clinical phenotype. *Invest Ophthalmol Vis Sci*. 2016;57(14):6033–6039.
10. Cremers FPM, van de Pol DJR, van Kerkhoff LPM, et al. Cloning of a gene that is rearranged in patients with choroideraemia. *Nature*. 1990;347(6294):674–677.
11. van Bokhoven H, van den Hurk JAJM, Bogerd L, et al. Cloning and characterization of the human choroideremia gene. *Hum Mol Genet*. 1994;3(7):1041–1046.
12. Andres DA, Seabra MC, Brown MS, et al. cDNA cloning of component A of Rab geranylgeranyl transferase and demonstration of its role as a Rab escort protein. *Cell*. 1993;73(6):1091–1099.
13. Patrício MI, Barnard AR, Xue K, MacLaren RE. Choroideremia: molecular mechanisms and development of AAV gene therapy. *Expert Opin Biol Ther*. 2018;18(7):807–820.
14. Seabra MC, Brown MS, Slaughter CA, Südhof TC, Goldstein JL. Purification of component A of Rab geranylgeranyl transferase: Possible identity with the choroideremia gene product. *Cell*. 1992;70(6):1049–1057.
15. Cremers FP, Armstrong SA, Seabra MC, Brown MS, Goldstein JL. REP-2, a Rab escort protein encoded by the choroideremia-like gene. *J Biol Chem*. 1994;269(3):2111–2117.
16. Larijani B, Hume AN, Tarafder AK, Seabra MC. Multiple factors contribute to inefficient prenylation of Rab27a in Rab prenylation diseases. *J Biol Chem*. 2003;278(47):46798–46804.
17. Wavre-Shapton ST, Tolmachova T, da Silva ML, Futter CE, Seabra MC. Conditional ablation of the choroideremia gene causes age-related changes in mouse retinal pigment epithelium. *PLoS One*. 2013;8(2):1–11.
18. Gordiyenko NV, Fariss RN, Zhi C, MacDonald IM. Silencing of the CHM gene alters phagocytic and secretory pathways in the retinal pigment epithelium. *Investig Ophthalmol Vis Sci*. 2010;51(2):1143–1150.
19. Futter CE, Ramalho JS, Jaissle GB, Seeliger MW, Seabra MC. The role of Rab27a in the regulation of melanosome distribution within retinal pigment epithelial cells. *Mol Biol Cell*. 2004;15(5):2264–2275.
20. Lopes VS, Ramalho JS, Owen DM, et al. The ternary Rab27a-Myrip-Myosin VIIa complex regulates melanosome motility in the retinal pigment epithelium. *Traffic*. 2007;8(5):486–499.
21. Lopes VS, Wasmeier C, Seabra MC, Futter CE. Melanosome maturation defect in Rab38-deficient retinal pigment epithelium results in instability of immature melanosomes during transient melanogenesis. Barr F, ed. *Mol Biol Cell*. 2007;18(10):3914–3927.
22. Meschede IP, Burgoyne T, Tolmachova T, Seabra MC, Futter CE. Chronically shortened rod outer segments accompany photoreceptor cell death in Choroideremia. Lewin AS, ed. *PLoS One*. 2020;15(11):e0242284.
23. Seabra MC, Ho YK, Anant JS. Deficient geranylgeranylation of Ram/Rab27 in choroideremia. *J Biol Chem*. 1995;270(41):24420–24427.
24. Köhnke M, Delon C, Hastie ML, et al. Rab GTPase prenylation hierarchy and its potential role in choroideremia disease. *PLoS One*. 2013;8(12):1–11.
25. El-Brolosy MA, Kontarakis Z, Rossi A, et al. Genetic compensation triggered by mutant mRNA degradation. *Nature*. 2019;568(7751):193–197.
26. Ma Z, Zhu P, Shi H, et al. PTC-bearing mRNA elicits a genetic compensation response via Upf3a and COMPASS components. *Nature*. 2019;568(7751):259–263.

27. Patricio MI, Barnard AR, Cox CI, et al. Biological activity of AAV vectors for choroideremia gene therapy can be measured by in vitro prenylation of RAB6A. *Mol Ther - Methods Clin Dev*. 2018;9:288–295.
28. Altschul SF, Gish W, Miller W, Myers EW, Lipman DJ. Basic local alignment search tool. *J Mol Biol*. 1990;215(3):403–410.
29. Jolly JK, Xue K, Edwards TL, Groppe M, MacLaren RE. Characterizing the natural history of visual function in choroideremia using microperimetry and multimodal retinal imaging. *Invest Ophthalmol Vis Sci*. 2017;58(12):5575–5583.
30. Edwards TL, Williams J, Patrício MI, et al. Novel non-contiguous exon duplication in choroideremia. *Clin Genet*. 2018;93(1):144–148.
31. Xue K, Jolly JK, Barnard AR, et al. Beneficial effects on vision in patients undergoing retinal gene therapy for choroideremia. *Nat Med*. 2018;24(10):1507–1512.
32. Edwards TL, Jolly JK, Groppe M, et al. Visual acuity after retinal gene therapy for choroideremia. *N Engl J Med*. 2016;374(20):1996–1998.
33. MacLaren RE, Groppe M, Barnard AR, et al. Retinal gene therapy in patients with choroideremia: initial findings from a phase 1/2 clinical trial. *Lancet*. 2014;383(9923):1129–1137.
34. Dimopoulos IS, Hoang SC, Radziwon A, et al. Two-year results after AAV2-mediated gene therapy for choroideremia: the Alberta Experience. *Am J Ophthalmol*. 2018;193:130–142.
35. Lam BL, Davis JL, Gregori NZ, et al. Choroideremia gene therapy phase 2 clinical trial: 24-month results. *Am J Ophthalmol*. 2019;197:65–73.
36. Fischer MD, Ochakovski GA, Beier B, et al. Changes in retinal sensitivity after gene therapy in choroideremia. *Retina*. 2020;40(1):160–168.
37. Seabra MC. New insights into the pathogenesis of choroideremia: a tale of two REPs. *Ophthalmic Genet*. 1996;17(2):43–46.
38. Sanchez-Alcudia R, Garcia-Hoyos M, Lopez-Martinez MA, et al. A comprehensive analysis of choroideremia: from genetic characterization to clinical practice. Janecke AR, ed. *PLoS One*. 2016;11(4):e0151943.
39. Sergeev YV., Smaoui N, Sui R, et al. The functional effect of pathogenic mutations in Rab escort protein 1. *Mutat Res - Fundam Mol Mech Mutagen*. 2009;665(1-2):44–50.